Communications

Ligand-Centered Oxidations and Electron Delocalization in a Tetranuclear Complex of a Tetradonor-Substituted Olefin

Michael Linseis,[†] Rainer F. Winter,[*,†] Biprajit Sarkar,[‡] Wolfgang Kaim,[‡] and Stanislav Záliš[§]

Institut für Anorganische Chemie, Universität Regensburg, Universitätsstrasse 31, 93040 Regensburg, Germany, Institut für Anorganische Chemie, Universität Stuttgart, Pfaffenwaldring 55, 70569 Stuttgart, Germany, and J. Heyrovský Institute of Physical Chemistry v. v. i., Academy of Sciences of the Czech Republic, Dolejškova 3, Prague, Czech Republic

Summary: The tetrakis(4-styryl)ethene ($TSTE^{4-}$)-bridged tetraruthenium complex $[\{(P^iPr_3)_2(CO)ClRu\}_4\{\mu_4\text{-}(CH=CHC_6H_4)_4(C=C)\}]$ undergoes four consecutive oxidations at low potential. The ligand-dominated nature of these processes is confirmed by spectroscopic and quantum-chemical investigations.

The ability of the easily reducible tetracyanoethylene (TCNE) ligand to bridge up to four metal centers and to adopt any oxidation state between 0 and −2 has generated a unique coordination chemistry[1,2] with potential applications in molecular magnetism, electrochromism, and molecular computing.[3,4] The coordination chemistry of electroactive, tetradonor-substituted olefins is much less explored but may hold similar potential. The tetrairon complex $[\{Cp^*(dppe)Fe^{II}\}_4\{\mu_4\text{-}(C\equiv CC_6H_4\text{-}4)_4(C=C)\}]$ of the (4-ethynylphenyl)ethene ligand $[(C\equiv CC_6H_4\text{-}4)_4C=C]^{4-}$ is a recent example.[5] This compound undergoes four consecutive metal-centered oxidations, during which the bridging ligand acquires only a small fraction δ of the positive charge(s): i.e., $[\{Cp^*(dppe)Fe^{II}\}_{4-n}\{Cp^*(dppe)Fe^{III-\delta/n}\}_n\{\mu_4\text{-}(C\equiv CC_6H_4\text{-}4)_4(C=C)\}^\delta]^{n+}$. Here we report on the tetraruthenium complex $[\{(P^iPr_3)_2(CO)ClRu\}_4\{\mu_4\text{-}(CH=CHC_6H_4)\}_4(C=C)\}]$ (**1**), which features the tetrakis(4-styryl)ethene ($TSTE^{4-}$) ligand (Chart 1).

Complex **1** was prepared as outlined in Scheme 1.[6] Treatment of the alkyne $(HC\equiv CC_6H_4)_4(C=C)$[7,8] with 4.08 equiv of $[HRu(CO)Cl(P^iPr_3)_2]$ gave **1** as a deep orange-red solid in 85% yield. ^1H NMR spectroscopy shows the presence of four equivalent vinyl groups with signals at δ 8.42 (H_α) and 5.90 (H_β) that display well-resolved H−H and P−H couplings of 13.4 and 0.9 Hz ($^2J_{P-H}$) and 2.1 Hz ($^3J_{P-H}$), respectively, and two signals of an AB system at δ 6.77 and 6.71 ppm for the *p*-phenylene groups. In ^{13}C NMR spectra the resonance signals of the ruthenium-bonded vinyl groups appear at 150.8 (C_α) and 134.8 ppm (C_β), again with well-resolved coupling to two equivalent phosphorus nuclei each. The central ethylene carbon atoms are observed at 139.8 ppm, while the phosphorus nuclei give rise to a sharp singlet at δ 38.3 ppm in $^{31}P\{^1H\}$ NMR spectroscopy (see Figure S1, Supporting Information).

The low $\tilde{\nu}(CO)$ value of 1909 cm^{-1} and the low oxidation potentials of **1** attest to its electron-rich character. Cyclic voltammetry of **1** shows two reversible couples at −0.020 and +0.415 V vs the ferrocene/ferrocenium standard (see Figure

* To whom correspondence should be addressed. E-mail: rainer.winter@chemie.uni-regensburg.de.
† Universität Regensburg.
‡ Universität Stuttgart.
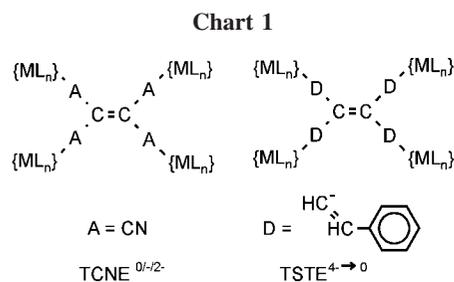§ J. Heyrovský Institute of Physical Chemistry v.v.i.
(1) Kaim, W.; Moscherosch, W. *Coord. Chem. Rev.* **1994**, *129*, 157.
(2) Miller, J. S. *Angew. Chem., Int. Ed.* **2006**, *45*, 2508.
(3) Miller, J. S.; Epstein, A. J. *Coord. Chem. Rev.* **2000**, *207*, 651.
(4) Wang, G.; Zhu, H.; Fan, J.; Slebodnik, C.; Yee, G. T. *Inorg. Chem.* **2006**, *45*, 1406.
(5) Tanaka, Y.; Ozawa, T.; Inagaki, A.; Akita, M. *Dalton Trans.* **2007**, 928.

Chart 1

A = CN

TCNE $^{0/-/2-}$

D =

TSTE$^{4- \to 0}$

S2, Supporting Information). Comparison of the slopes of i vs $t^{1/2}$ plots in chronoamperometry and of the step heights in steady-state voltammetry to those of decamethylferrocene according to the method of Baranski[9] established that each anodic couple involves the transfer of *two* electrons. The peak-to-peak separations, particularly of the first couple, are notably smaller than that of decamethylferrocene under identical conditions. This signals that there is only a small splitting between the first and the second oxidations underlying the first wave and between the third and the fourth oxidations that give rise to the second wave. Similar behavior has been noted for metal-free tetrakis(4-dimethylaminophenyl)ethene.[10] Half-wave potentials as determined by digital simulation[11] are −0.028 V (0 → +), −0.013 V (+ → 2+), 0.400 V (2+ → 3+), and 0.434 V (3+ → 4+), from which comproportionation constants $K_{c,1}$ = 1.8 ± 0.2, $K_{c,2}$ = (9.6 ± 0.8) × 10^6, and $K_{c,3}$ = 3.8 ± 0.6 are calculated (eqs 1–4).

$$\mathbf{1^{2+}} + \mathbf{1^0} \overset{K_{c,1}}{\rightleftharpoons} 2\mathbf{1^+} \qquad (1)$$

$$\mathbf{1^{3+}} + \mathbf{1^+} \overset{K_{c,2}}{\rightleftharpoons} 2\mathbf{1^{2+}} \qquad (2)$$

$$\mathbf{1^{4+}} + \mathbf{1^{2+}} \overset{K_{c,3}}{\rightleftharpoons} 2\mathbf{1^{3+}} \qquad (3)$$

$$K_c = \exp{(nF\Delta E_{1/2}/RT)} \qquad (4)$$

Stepwise oxidation inside a thin-layer electrolysis cell induced a blue shift of the CO band of **1** during the conversion of the neutral form to the dication $\mathbf{1^{2+}}$ and its

(6) All synthetic work was performed with dry solvents under a dry nitrogen atmosphere. Synthesis of **1**: a solution of 97 mg (0.227 mmol) of tetrakis(4-ethynylphenyl)ethene in 10 mL of CH$_2$Cl$_2$ was added dropwise with stirring to a solution of 450 mg (0.926 mmol) of [HRu(CO)Cl(PiPr$_3$)$_2$] in 10 mL of CH$_2$Cl$_2$. After addition was complete, the solution was concentrated to 1.5 mL under vacuum and 25 mL of methanol was added. The resulting red solid was isolated by filtration, washed with three 5 mL portions of methanol, and dried under vacuum to give 457 mg (0.192 mmol, 84.7%) of **1** as a red powder. Selected spectroscopic data of complex **1**: ^{1}H NMR (400 MHz, CD$_2$Cl$_2$, 298 K) δ 8.42 (dt, 4H, $^3J_{H-H}$ =13.4 Hz, $^3J_{P-H}$ = 0.9 Hz, Ru−CH), 6.77, 6.71 (each d, 8H, $^3J_{H-H}$ = 8.2 Hz, C$_6$H$_4$), 5.90 (dt, 4H, $^3J_{H-H}$ = 13.4 Hz, $^4J_{P-H}$ = 2.1 Hz, Ru−CH=C*H*), 2.74 (m, 24H, PC*H*(CH$_3$)$_2$), 1.29 (m, 144H, PCH(C*H$_3$*)$_2$); ^{13}C NMR (100.6 MHz, CD$_2$Cl$_2$, 298 K): δ 203.4 (t, $^2J_{P-C}$ = 13.1 Hz, CO), 150.8 (t, $^2J_{P-C}$ = 10.8 Hz, Ru−CH), 140.5 (s, C=C*C*), 139.8 (s, *C*=C), 137.0 (t, $^4J_{P-C}$ = 2.0 Hz, Ru−CH=CH*C*), 134.8 (t, $^3J_{P-C}$ = 3.4 Hz, Ru−CH=*C*H), 131.7, 123.3 (each s, CH styryl), 24.8 (vt, J_{P-C} = 9.8 Hz, P*C*H(CH$_3$)$_2$), 21.1, 19.9 (each s, CH(*C*H$_3$)$_2$); ^{31}P{^{1}H} NMR (CD$_2$Cl$_2$, 121.5 MHz, 298 K) δ 38.3 (s); IR (KBr, $\tilde{\nu}$ in cm^{-1}): 2962, 2930, 2873 (m, $\tilde{\nu}_{CH}$), 1909 (s, $\tilde{\nu}_{CO}$), 1598, 1567, 1536, 1504 (m, $\tilde{\nu}_{C=C}$, aryl, vinyl, ethene); UV/vis (CH$_2$Cl$_2$, λ_{max} (ε_{max} in L mol^{-1} cm^{-1})) 312 (sh, 47 000), 352 (86 000), 400 (sh, 46 000), 525 (2800). Anal. Calcd (found) for C$_{110}$H$_{192}$Cl$_4$O$_4$P$_8$Ru$_4$: C, 55.69 (55.43); H, 8.16 (8.53).

(7) Sengupta, S. *Synlett* **2004**, 1191.

(8) Tanaka, K.; Hiratsuka, T.; Kojima, Y.; Osano, Y. T. *J. Chem. Res., Synop.* **2002**, 209.

(9) Baranski, A. S.; Fawcett, W. R.; Gilbert, C. M. *Anal. Chem.* **1985**, 57, 166.

(10) Phelps, J.; Bard, A. J. *J. Electroanal. Chem. Interfacial Electrochem.* **1976**, 68, 313.

(11) Rudolph, M.; Feldberg, S. DigiSim3, Version 3.03, DigiSim3, Version 3.03; Bioanalytical Systems, Inc.,1994.

further conversion to fully oxidized $\mathbf{1^{4+}}$ (Figure 1). There is only one CO band for **1** ($\tilde{\nu}$(CO) 1909 cm^{-1}) and $\mathbf{1^{4+}}$ ($\tilde{\nu}$(CO) 1968 cm^{-1}) but a broad asymmetric band for $\mathbf{1^{2+}}$. According to spectral deconvolution this band results from overlapping individual absorptions at 1924 and 1942 cm^{-1} (Supporting Information, Figure S3). Any combination of two out of the three pathways of electron delocalization in such systems (diagonal, lateral, or cross conjugation,; see Chart S1 of the Supporting Information) would render each of the four styryl ruthenium moieties equivalent.[7,12,13] The presence of two pairs of electronically different carbonyl ruthenium moieties in $\mathbf{1^{2+}}$ thus signals that only one of these pathways is effective on the fast IR time scale of about 10^{-12} s. The overall CO band shift of 57 cm^{-1} between neutral **1** and fully oxidized $\mathbf{1^{4+}}$ is significantly smaller than that of ca. 130−150 cm^{-1} that would be expected of a metal-centered oxidation process and that of 81 cm^{-1} for [{(P^{i}Pr$_3$)$_2$(CO)ClRu}$_2$(μ-CH=CHC$_6$-H$_4$CH=CH-1,4)],[14] where also one electron per vinyl ruthenium moiety is released. This is a consequence of the more extended π-chromophore of **1**, which leads to an exceptionally strong ligand contribution to the redox orbitals.

The comproportionation constant of one-electron-oxidized $\mathbf{1^+}$, while small at $K_{c,1}$ = 1.8 ± 0.2, is still large enough to allow for its detection by ESR spectroscopy. The room-temperature ESR spectrum (Supporting Information, Figure S4) consists of an unresolved isotropic signal at g = 2.0157. When the temperature is lowered to 110 K, a rhombic splitting of the **g** tensor is observed with individual **g** tensor components g_x = 2.072, g_y = 2.034, and g_z = 2.014 ($\langle g_{av} \rangle$ = 2.040, Δg = 0.058). This characterizes $\mathbf{1^+}$ as a metal-stabilized but mainly ligand-centered paramagnetic species, as is also the case for other vinyl ruthenium complexes with π-conjugated substituents attached to the vinyl group.[14–16]

In the electronic spectrum of **1** the bands of parent tetrakis(4-ethynylphenyl)ethene[8] are preserved but undergo a bathochromic shift of 8100 and 4100 cm^{-1}, respectively (Supporting Information, Figure S5). This goes along with an approximate doubling in molar absorptivity. Both these observations point to efficient electronic conjugation across the entire organometallic chromophore. Upon oxidation to the dication $\mathbf{1^{2+}}$ the 390 nm band of **1** decreases in intensity and is gradually replaced by intense, broad absorptions that extend over the low-energy part of the optical spectrum and the near-IR. Distinct maxima are observed at 8400, 13 680, and 15 080 cm^{-1} (Figure 2). The intermediate radical monocation, while not separately detected in this regime, gives rise to a characteristic absorption at about 4730 cm^{-1} which intensifies during the initial stages of the electrolysis and then gradually disappears, while the absorption bands of $\mathbf{1^{2+}}$ continue to grow (Supporting Information, Figure S6). Further oxidation with slow scanning through the second wave generates the tetracation $\mathbf{1^{4+}}$. It is another strongly absorbing species with peak maxima at 11 610, 14 870, and 17 660 cm^{-1} and thus has energies distinctly higher than those of the corresponding dication but considerably lower energies in comparison to those

(12) Hilger, A.; Gisselbrecht, J.-P.; Tykwinski, R. R.; Boudon, C.; Schreiber, M.; Martin, R. E.; Lüthi, H. P.; Gross, M.; Diederich, F. *J. Am. Chem. Soc.* **1997**, *119*, 2069.

(13) Giuffreda, M. G.; Bruschi, M.; Lüthi, H. P. *Chem. Eur. J.* **2004**, *10*, 5671.

(14) Maurer, J.; Sarkar, B.; Schwederski, B.; Kaim, W.; Winter, R. F.; Záliš, S. *Organometallics* **2006**, *25*, 3701.

(15) Maurer, J.; Winter, R. F.; Sarkar, B.; Fiedler, J.; Záliš, S. *Chem. Commun.* **2004**, 1900.

(16) Maurer, J.; Linseis, M.; Sarkar, B.; Schwerderski, B.; Niemeyer, M.; Kaim, W.; Záliš, S.; Anson, C.; Zabel, M.; Winter, R. F. *J. Am. Chem. Soc.* **2008**, *130*, 259.

Scheme 1. Synthesis of Complex 1

i) Me₃SiCCH, PdCl₂(PPh₃)₂, NEt₃; ii) NH₄F, THF, MeOH

iii) HRu(CO)Cl(P^{i}Pr₃)₂, CH₂Cl₂
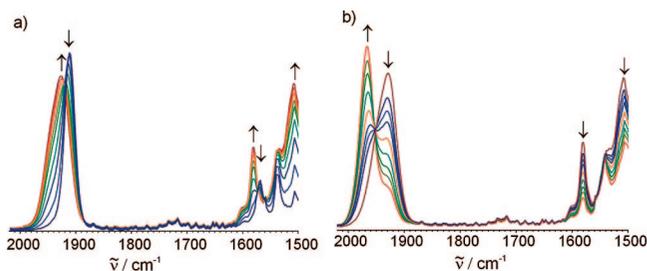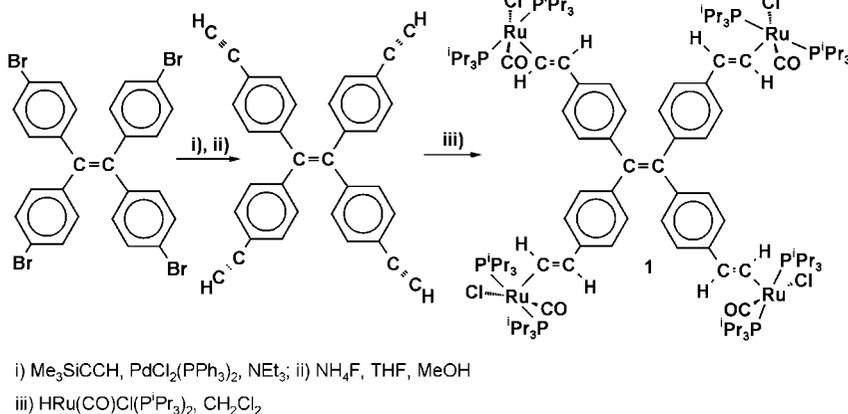
Figure 1. IR spectroelectrochemistry of complex **1** in 1,2-C₂H₄Cl₂/NBu₄PF₆: spectroscopic changes upon oxidation (a) of **1** to **1²⁺** and (b) of **1²⁺** to **1⁴⁺**.
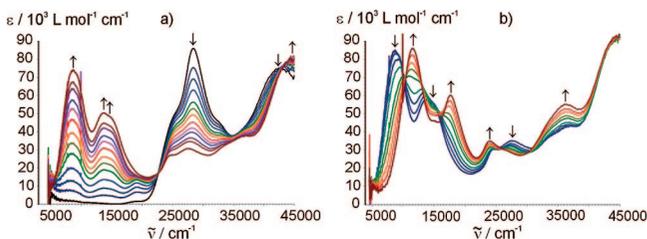
Figure 2. UV/vis/near-IR spectroelectrochemistry of complex **1** in 1,2-C₂H₄Cl₂/NBu₄PF₆: spectroscopic changes upon oxidation (a) of **1** to **1²⁺** and (b) of **1²⁺** to **1⁴⁺**.

of neutral **1** (Figure 2). The intermediate trication **1³⁺** is also observed by virtue of a low-energy absorption at 5060 cm⁻¹ at the border of the near-IR and mid-IR regions (Supporting Information, Figure S7). Stepwise reduction at any stage restored neutral **1** such that the **1** ⇌ **1²⁺** ⇌ **1⁴⁺** redox system constitutes a reversible cycle. The stepwise oxidation of mainly the bridging ligand makes **1** a strongly chromophoric organometallic violene/cyanine hybrid[17] with a delocalized π system and a large number of closely spaced occupied energy levels below the HOMO.

Quantum chemical density functional (DFT) calculations on the simplified PH₃-substituted model **1′** were conducted in order to understand the structural, electronic, and spectroscopic properties and their dependence on the overall oxidation state.[18–22] Stepwise oxidation of tetraarylethenes to their dica-

tions induces a large torsion of the Ar₂C moieties around the central CC bond, a coplanar arrangement of at least one aryl ring with the plane defined by the central carbon and the attached ipso carbon atoms of each CAr₂ subunit, and quinoidal distortion of the aryl subsituents.[23,24] DFT-optimized structures of model complex **1′** and its various oxidized forms (Supporting Information, Figure S8 and Table S1) show that TSTE⁴⁻-bridged tetraruthenium complexes behave in the same manner. The central CC bond lengthens from 1.371 Å in **1′** to 1.458 Å in the dication **1′²⁺** and to 1.484 Å in the tetracation **1′⁴⁺**. This is accompanied by an increasing deviation of the central ethylene group from planarity and a concomitant decrease of the torsional angles between the methylene planes and the planes of the attached aryl rings. Vibrational analysis of **1′** and oxidized **1′²⁺** and **1′⁴⁺** reproduces the average CO band shifts (28 cm⁻¹ vs 24 cm⁻¹ for the first oxidation, 33 cm⁻¹ vs 35 cm⁻¹ for the second oxidation) and the presence of two separate, intense absorptions for **1′²⁺** but underestimates the experimental splitting (5 cm⁻¹ vs 18 cm⁻¹) (Supporting Information, Table S2). The calculations on **1′²⁺** also indicate that the geminally disposed styryl moieties A and B on one hand and C and D on the other hand are pairwise equivalent but different from the other pair (Supporting Information, Figure S8). This suggests that the geminal delocalization pathway is the most efficient one.

Figure 3 shows that the highest occupied molecular orbital (HOMO) of **1′** is delocalized across the π system of the bridging ligand with smaller contributions from Ru 4d$_{xz}$ orbitals (12%). The closely lying HOMO-1, HOMO-2, and HOMO-3 orbitals have negligible contributions from the central ethylene group and are mainly composed of the styryl π orbitals with overall Ru contributions of 28, 30, and 36%, respectively. The LUMO of **1** is an antibonding combination of π orbitals of the bridging ligand (6% Ru) (Supporting Information, Figure S9).

TD DFT calculations on **1²⁺** retrace the main features of the experimental electronic spectrum well, although transition energies are somewhat overestimated (Supporting Information, Figure S10). Intense low-energy transitions b¹A and c¹A correspond mainly to the excitations HOMO → LUMO and HOMO-2 → LUMO of **1²⁺**, respectively. The composite low-energy band can thus be characterized as involving both π → π* and MLCT components. The band h¹A calculated at around

(17) Hünig, S.; Kemmer, M.; Wenner, H.; Barbosa, F.; Gscheidt, G.; Perepichka, I. F.; Bäuerle, P.; Emge, A.; Peters, K. *Chem. Eur. J.* **2000**, *6*, 2618.

(18) The hybrid B3LYP functional[19] together with 6-31G* polarized double-ζ basis sets[20] for C, N, H, and O atoms and effective core pseudopotentials and corresponding optimized sets of basis functions for Ru atoms[21] were used in DFT calculations.[22] Frequency analysis and TD DFT calculations were done at optimized structures.

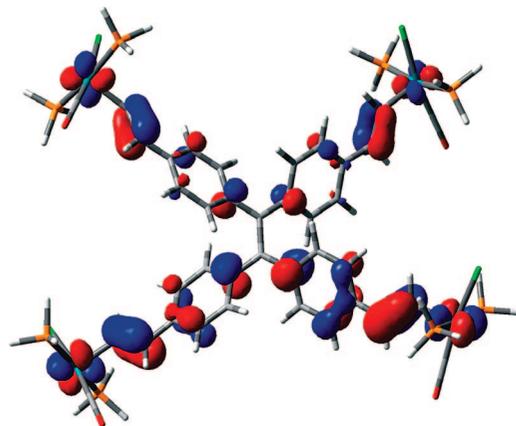(19) Becke, A. D. *J. Chem. Phys.* **1993**, *98*, 5648.

(20) Hariharan, P. H.; Pople, J. A. *Theor. Chim. Acta* **1973**, *28*, 213.

(21) Andrae, D.; Haeussermann, U.; Dolg, M.; Stoll, H.; Preuss, H. *Theor. Chim. Acta* **1990**, *77*, 123.

(22) Gaussian 03, Revision C.02; www.gaussian.com.

(23) Rathore, R.; Lindeman, S. V.; Kumar, A. S.; Kochi, J. K. *J. Am. Chem. Soc.* **1998**, *120*, 6931.

(24) Bock, H.; Näther, C.; Havlas, Z. *J. Chem. Soc., Chem. Commun.* **1995**, 1111.

Figure 3. Contour plot of the HOMO of **1**.

19 000 cm^{-1} is assigned as the excitation from the HOMO-1 to the LUMO+1 of $\mathbf{1^{2+}}$.

In summary, we have prepared the organometallic tetrakis(4-styryl)ethene tetraanion (TSTE^{4-})-bridged tetraruthenium complex **1**, which undergoes a series of four reversible ligand-centered oxidations. The low oxidation potentials and the reversibility of all oxidation processes are a further demonstration of the impressive stabilizing effect of vinyl ruthenium moieties on organic π systems, rivaling that of the dimethyl-amino group. Moreover, the $\mathbf{1 \rightleftarrows 1^{2+} \rightleftarrows 1^{4+}}$ redox series constitutes a strongly electrochromic[25–27] system with high absorptivities in the low-energy part of the visible and the near-infrared (near-IR) regions at the dication and tetracation levels.

Supporting Information Available: Figures showing the ^{1}H, ^{13}C, and ^{31}P NMR spectra, the cyclic voltammogram, and the spectral deconvolution of the IR band of $\mathbf{1^{2+}}$, ESR spectra of $\mathbf{1^{+}}$, UV/vis spectra of **1** and its parent alkyne, vis/near-IR spectra showing the presence of the $\mathbf{1^{+}}$ and $\mathbf{1^{3+}}$ intermediates, a comparison of the TD-DFT calculated and experimental electronic spectra of $\mathbf{1^{2+}}$, selected frontier orbitals of **1′**, and a chart with possible pathways of electron delocalization in $\mathbf{1^{2+}}$ and tables with calculated structure parameters and $\tilde{\nu}$(CO) values of **1′** in its various oxidation states. This material is available free of charge via the Internet at http://pubs.acs.org.

OM8003338

(25) Monk, P. M. S.; Mortimer, R. J.; Kosseinsky, D. R. *Electro-chromism*; VCH: Weinheim, Germany, 1995.
(26) Mortimer, R. J. *Chem. Soc. Rev.* **1997**, *26*, 147.
(27) Ward, M. D. *J. Solid State Electrochem.* **2005**, *9*, 778.